The DOE Water Cycle Pilot Study

N.L. Miller[1]*, A.W. King[2], M.A. Miller[3], E.P. Springer[4], M.L. Wesely[5],

K.E. Bashford[1], M.E. Conrad[1], K. Costigan[4], P.N. Foster[1], H.K. Gibbs[2], J. Jin[1], J. Klazura[5],

B.M. Lesht[5], M.V. Machavaram[1], F. Pan[2], J. Song[5#], D. Troyan[3], R.A. Washington-Allen[2]

Bulletin of the American Meteorological Society

Submitted 24 September 2003

Accepted with Revisions 30 March 2004

Resubmitted 8 June 2004

* Corresponding Author: Norman L Miller; nlmiller@lbl.gov;

90-1116 One Cyclotron Road, Earth Sciences Division,

Lawrence Berkeley National Laboratory, Berkeley, California 94720

[1] LBNL, Lawrence Berkeley National Laboratory, Berkeley, California

[2] ORNL, Oak Ridge National Laboratory, Oak Ridge, Tennessee

[3] BNL, Brookhaven National Laboratory, Upton, New York

[4] LANL, Los Alamos National Laboratory, Los Alamos, New Mexico

[5] ANL, Argonne National Laboratory, Argonne, Illinois

[#] ANL Research Affiliate and Northern Illinois University, DeKalb, Illinois

ABSTRACT

A Department of Energy (DOE) mutli-laboratory Water Cycle Pilot Study (WCPS) investigated components of the local water budget at the Walnut River Watershed in Kansas to study the relative importance of various processes and to determine the feasibility of observational water budget closure. An extensive database of local meteorological time series and land surface characteristics was compiled. Numerical simulations of water budget components were generated and, to the extent possible, validated for three nested domains within the Southern Great Plains; the DOE Atmospheric Radiation Measurement/Cloud Atmospheric Radiation Testbed (ARM/CART), the Walnut River Watershed (WRW), and the Whitewater Watershed (WW), Kansas

A 2-month Intensive Observation Period (IOP) was conducted to gather detailed observations relevant to specific details of the water budget, including fine-scale precipitation, streamflow, and soil moisture measurements not made routinely by other programs. Event and seasonal water isotope ($\delta^{18}O$, δD) sampling in rainwater, streams, soils, lakes, and wells provided a means of tracing sources and sinks within and external to the WW, WRW, and the ARM/CART domains. The WCPS measured changes in leaf area index for several vegetation types, deep groundwater variations at two wells, and meteorological variables at a number of sites in the WRW. Additional activities of the WCPS include code development toward a regional climate model with water isotope processes, soil moisture transect measurements, and water level measurements in ground water wells.

1. Introduction

In 1999, the U.S. Global Change Research Program (USGCRP) formed a Water Cycle Study Group (Aber et al. 1999) to organize research efforts in regional hydrologic variability, the extent to which this variability is caused by human activity, and the influence of ecosystems. The USGCRP Water Cycle Study Group was followed by a U.S. Department of Energy (DOE) Water Cycle Research Plan (DOE 2002) that outlined an approach toward improving seasonal to inter-annual hydroclimate predictability and closing a regional water budget. The DOE Water Cycle Plan identified key research areas, including a comprehensive long-term observational database to support model development, and a better understanding of the relationship between the components of local water budgets and large scale processes. In response to this plan, a multi-laboratory DOE Water Cycle Pilot Study (WCPS) demonstration project began with a focus on studying the water budget and its variability at multiple spatial scales.

Previous studies have highlighted the need for continued efforts to observationally close a local water budget, develop numerical model closure, and to further quantify the scales in which predictive accuracy are optimal. A concerted effort within the NOAA-funded Global Energy and Water Cycle Experiment (GEWEX) Continental-scale International Project (GCIP) put forth a strategy to understand various hydrometeorlogical processes and phenomena with an aim toward closing the water and energy budgets of regional watersheds (Lawford 1999, 2001). The GCIP focus on such regional budgets includes measurement of all components and reducing the error in the budgets to near-zero. To approach this goal, quantification of the uncertainties in both measurements and modeling is required. Model uncertainties within regional climate models continue to be evaluated within the Program to Intercompare Regional Climate Simulations (Takle et al. 1999), and model uncertainties within Land Surface Models are being evaluated within the

Program to Intercompare Land Surface Schemes (e.g. Henderson-Sellers 1993, Wood et a. 1998; Lohmann et al. 1998).

In the context of understanding the water budget at watershed scales, two research questions that highlight DOE's unique water isotope analysis and high performance modeling capabilities were posed as the drivers of this pilot study:

1) Can the predictability of the regional water budget be improved using high-resolution model simulations that are constrained and validated with new hydrospheric water measurements?

2) Can water isotopic tracers be used to segregate different pathways through the water cycle and predict a change in regional climate patterns?

To address these questions, numerical studies using regional atmospheric-land surface models and multi-scale land surface hydrologic models were generated and, to the extent possible, the results were evaluated with observations. While the number of potential processes that may be important in the local water budget is large, several key processes were examined in detail. Most importantly, a concerted effort was made to understand water cycle processes and feedbacks at the land surface-atmosphere interface at spatial scales ranging from 30 meters to 100's of km.

A simple expression for the land surface water budget at the watershed scale is expressed as,

$$\Delta S = P + G_{in} - ET - Q - G_{out} \quad (1)$$

ΔS is the change in water storage, P is the precipitation, ET is the evapotranspiration, Q is streamflow, G_{in} is groundwater entering the watershed, and G_{out} is groundwater leaving the watershed, per unit time.

The WCPS project identified data gaps and necessary model improvements that will lead to a more accurate representation of the terms in Eq. 1. Table 1 summarizes the components of this water cycle pilot study and the respective participants. The following section provides a description of the surface observation and modeling sites. This is followed by a section on model analyses, and then the summary and concluding remarks.

Table 1 HERE

2. Site Description

The Walnut River Watershed (WRW) located in south-central Kansas is about 6000 km^2, is an order of magnitude smaller than the Atmospheric Radiation Measurement/Cloud Atmospheric Radiation Testbed (ARM/CART) site within which it is contained (Fig. 1). The major streams in the WRW are the Walnut River and its tributary, the Whitewater River. The two major reservoirs on the river system are El Dorado Lake and Winfield Lake. Surface water represents 91% of the water used in the WRW. Over 77% of the water use in WRW is for municipal purposes, with 10% for irrigation, 6.4% recreational use, and 3.3% industrial use (Kansas Water Office, 1997).

This watershed is a partially closed basin (Karst geology prevents full closure) amenable to computing the components of the hydrological budget, and is sufficiently small to allow reasonable observational coverage while having heterogeneous land cover types. The 1050 km^2 Whitewater Watershed (WW) is located in the northwest portion of the WRW, and within the WW is the 12 km^2 Rock Creek (RC). These sub-domains were selected for detailed observations and scaling

studies partly because there are ongoing and previous studies here providing data and related information (LeMone et al. 2000).

The WRW has strong east-west terrain, precipitation, vegetation, and geological gradients. The surface elevation drops from about 500 m in the east to about 330 m in the southwest. Average precipitation in the eastern region is 86 cm/yr, and the western region is 76 cm/yr. Approximately 65% of the precipitation falls between April and September, with an annual-average snowfall of about 35 cm snow water equivalent. The Walnut River floods once a year on average, downstream of the town of Towanda (Fig. 1). Land use in the WW is approximately 65% cropland and 32% grassland, with the eastern region grassland, and the western region primarily cropland with urban expansion from nearby Wichita.

Figure 1 a and b. HERE

3. Data Measurements and Sampling

Participants in the WCPS compiled an extensive database from archives (meteorology, vegetation types, topographic maps) and data obtained during a 1 April to 30 June 2002 Intensive Observation Period (IOP). In addition, the WCPS conducted event and seasonal sampling and periodic vegetation mapping. Models were evaluated at three nested domains; the ARM/CART, the WRW, and the WW, (Fig. 1). In the subsections that follow, observations of components of the water budget in all three domains are presented. The observations consist of satellite retrievals of the Leaf Area Index (LAI), which is a critical parameter in the evapotransipration term in Eq.1, measurements from local wells, which help constrain the groundwater terms in Eq. 1, and water isotopic tracers, which segregate water samples by physical process.

3.1. Leaf Area Index Measurements

Latent heat flux and surface albedo are sensitive to vegetation distribution, where the former is modulated by the valve-like action of the leaf stomata and the latter by the scattering characteristics of the leaf chlorophyll and leaf chemical composition. Both are intrinsically tied to the Leaf Area Index (LAI), and should be represented accurately in water cycle models. In this study, spatially extensive ground-based measurements were collected on 111 plots (row crops, woodland, grassland, and pasture) across the entire WW in July 2002. The plots were 900 m^2 for comparison with the Landsat TM/ETM+ 30 m resolution.

The spatial distribution of LAI was estimated from satellite data using empirical relationships between the measured LAI and the Normalized Difference Vegetation Index (NDVI) derived from above-canopy measurements of reflectance obtained with a field radiometer. LAI-NDVI relationships were first established for three of the four vegetation types (row crops, grassland, and pasture) and for variations of these types, combined statistically fitting measured LAI values to the corresponding NDVI values. Lack of canopy access precluded field measurement of woodland reflectance. The LAI-NDVI relationships were then applied to NDVI derived from the Landsat TM/ETM+ data, producing high-resolution LAI maps for WW.

Measured LAI values varied greatly within each vegetation type, with LAI-NDVI regressions (r^2) values ranging from 0.66 to 0.78 for each vegetation type and for all types combined. Figure 2 shows LAI predicted for July 2002 from the LAI-NDVI relationship combining measurements for all cropland, grassland and pasture plots. The 30 m resolution of the Landsat ETM+ data describes the spatial heterogeneity of LAI in the WW, with the spatially-explicit LAI values well within the statistical distributions of field observations (Table 2).

Table 2. HERE

Figure 2. HERE

In July 2002, LAI across the WW varied spatially within each vegetation type from nearly bare ground to full canopy (Table 2). Accordingly, based on the model results for minimum (10^{th} percentile) and maximum (90^{th} percentile) LAI, the within-vegetation spatial LAI variability may result in spatial latent heat flux variability within a vegetation type as high as 400 W m^{-2} at mid-day (Fig. 3). For comparison, this spatial variability in both LAI and latent heat flux is comparable to the seasonal variability that might be observed for a warm mesic deciduous/cropland system. This analysis reinforces the need for accurate characterizations of spatial LAI variability to accurately simulate the fine-scale spatial Latent heat flux variability.

Figure 3. HERE

3.2. Groundwater Well and Soil Moisture Transect Measurements

The location of groundwater affects the energy balance and the exchange of latent heat because deeper-rooted vegetation may have access to this water, and the long term soil moisture memory is linked to the deeper zone (Maxwell and Miller 2004). In the absence of surface reservoirs, groundwater also flows at a much slower rate than the other water fluxes in the budget equation (Eq. 1). As such, groundwater exhibits hysteresis in the local water cycle. Groundwater measurements performed for the WCPS represent a cursory attempt to provide insight into the groundwater response for the study period.

The hourly water elevation change in three wells (Potwin, B295, A272) for May 2002 to March 2003 are shown in Fig. 4 (a-c). Water level fluctuations in these wells are on the order of 0.3 m or less. An indication of the annual cycle in groundwater elevation can be seen in Figures 4 b and c, but longer time series are needed to quantify the relationship between the local climate and groundwater response. Most importantly, the three dimensional groundwater flow characteristics across the various domains examined in this study are unknown due to cost-constrained under-sampling. Without a comprehensive groundwater measurement program, specification of the groundwater terms in the water budget is virtually impossible.

Figure 4 HERE

One set of soil moisture measurements was made during the week of 6-8 May 2002 on recently tilled milo and wheat fields. A grid with a spacing of 30 m was sampled at 0.3 m spacing and at approximately 10 cm depth to examine small-scale variability. On the RC site, transects on the north side of the channel were established for surface soil moisture measurements on successive days between 5 and 7 June 2002.

Statistical analysis reveals a general drying of the area over the three days of observation. The mean soil moisture values [$cm^3 cm^{-3}$] were 0.54, 0.51, and 0.49 for 5, 6, and 7 June, respectively (Fig. 5). The standard deviation increases from 3.59 on 5 June to 4.00 on 6 June, and 5.20 on 7 June. Again, these data represent a limited snapshot of the surface soil moisture distribution in the Whitewater River Basin but provide some points of reference to check results of the simulation models.

Figure 5. Here

3.3 Water Isotopic Monitoring and Sampling

The stable hydrogen and oxygen isotope ratios of atmospheric moisture vary depending on the source of the water, the extent of precipitation loss, and physical parameters such as temperature and humidity. These relationships provide a critical link between local water cycle processes and the larger climate system. Isotope sampling helps quantify terms in the water budget equation, while at the same time providing information on the historical movement of water that is currently a component of the local water cycle.

As part of the WCPS, an extensive study of the isotopic compositions of all components of the water cycle in the WRW was conducted. This work included event-based precipitation sampling (consisting of one or more samples of every significant storm) at two sites within the WRW. Samples of selected precipitation events were also collected from four other sites in the WRW to examine the spatial variability of precipitation at the watershed scale. To determine the isotopic composition of storm systems and related large scale climate variations affecting the WRW, precipitation samples from 10 National Atmospheric Deposition Program (NADP) stations located along the primary storm tracks impacting the WRW were obtained. Additionally, water isotope samples of near-surface atmospheric vapor, surface water bodies, soil moisture, and ground water were and are collected every 3 to 4 months to monitor the response of isotopic compositions of components of the water cycle to seasonal and spatial variations in precipitation. During the IOP, a series of atmospheric vapor samples were collected at elevations up to 4000 m above the land surface to examine mixing between locally derived water vapor and moisture aloft. A detailed study of isotopic variations in a small tributary of the Whitewater River in response to two intense

storm events was also undertaken to quantify the response of streamflow to specific precipitation events (Machavaram et al., 2004).

In general, the δD and $\delta^{18}O$ values of storm systems decrease with distance from the source (primarily the Gulf of Mexico in this case), reflecting the progressive loss of higher δD and $\delta^{18}O$ precipitation. However, the isotopic compositions of precipitation are also affected by the addition of moisture from other sources including evaporation of surface water and mixing with moisture from other storm tracks. The effect of secondary moisture from evapotranspiration can be estimated from changes in the deuterium-excess of atmospheric vapor and precipitation. Initial isotopic measurements of the NADP and WRW rain samples show a systematic increase in the deuterium-excess of precipitation as storms move from the Gulf of Mexico region northward into the WRW. Conversely, moisture derived from the high-latitude jet stream causes significant drops in δD and $\delta^{18}O$ values of precipitation, especially during the colder winter months.

Fig. 6a contains volume-weighted oxygen isotope ratios ($\delta^{18}O$) for precipitation samples collected from one site in the WRW. In general, the $\delta^{18}O$ values range from approximately -4‰ in the summer to -10‰ in the winter. However, the isotope data also vary in response to significant differences in the weather from one year to the next. In July - August 2001, mean temperatures were almost 3°C higher than during July - August 2002. Despite nearly identical rainfall totals, the average $\delta^{18}O$ and deuterium-excess values of the precipitation were significantly higher in 2001 (2.5‰ and 5‰, respectively), reflecting the increased role of moisture derived from the land surface during the warmer weather. Conversely, the mean temperature during October - November 2002 was 4°C lower than during October - November 2001 and there was unusually high precipitation during October 2002 (more than 3 times normal). The average $\delta^{18}O$ values of the precipitation samples collected during this period were approximately 1.5‰ lower than during

October 2001, indicating a significant input of cold Arctic moisture derived from the high-latitude jet stream.

Both the general precipitation patterns and the extreme events also cause measurable shifts in the isotopic compositions of the rivers in the WRW (Fig. 6b). The $\delta^{18}O$ values of the Whitewater ranged between -4.4‰ and -5.9‰, with the summer samples greater than -5‰ and the winter samples less than -5.7‰, reflecting the general seasonal variations in precipitation. However, the two samples collected in the fall differed by 1.4‰ as a direct result of the intense, cold, low-$\delta^{18}O$ storm system in October 2002. The $\delta^{18}O$ values of the Walnut River above its confluence with the Whitewater River were not strongly influenced by the precipitation because this section is primarily fed by water from the El Dorado Reservoir that has been shifted to higher $\delta^{18}O$ values due to evaporation. Because of the size of the reservoir, this water dominates flow in the Walnut River, causing its $\delta^{18}O$ values to remain relatively constant at -2.8 to -3.5‰. Downstream of the Whitewater River, the $\delta^{18}O$ value of the water is a mixture of the two signals, with the proportions varying due to the intensity of storm activity and the amount of water released from El Dorado reservoir. For example, during October 2002 the $\delta^{18}O$ value of the lower Walnut River was closer to the $\delta^{18}O$ value of the Whitewater River due to the high precipitation levels during the fall of that year.

Figure 6. Here

These data demonstrate the sensitivity of the isotope compositions of water to climatic factors impacting the water cycle. The regional precipitation data highlight the impacts of deviations from normal temperatures on the water cycle. Systematic changes in temperature due to

factors such global climate change should be readily recognizable. Monitoring the isotopic compositions of rivers and lakes provides a good, long-term average of precipitation patterns, modified by the effects of evaporation from the lakes (reservoirs) and infiltration of soil water. This also presents a potential monitor of the impacts of land-use changes (e.g., building reservoirs, increased crop irrigation, changes in vegetation) on the local water cycle. Ultimately, however, the most beneficial use of isotope monitoring will be to validate numerical simulations of the water cycle in order to enable the use of these models for long-term predictions of the climate patterns.

4. Modeling and Analysis

Mesoscale models provide a medium for comprehensive understanding of the processes that operate in the local water cycle, as well as predictive capability. There have been a limited number of studies designed to evaluate the efficacy of the water cycle-related parameterizations used in mesoscale models, as well as tests of the sensitivity of the models to resolution (vertical and horizontal). In this section, parameterizations in a coupled atmosphere-land-surface model are compared to observations and resolution sensitivity is tested. In addition to these analyses, code development on the implementation of stable water isotopes in a regional climate model is also discussed.

4.1. Coupled Mesoscale Atmospheric-Land Surface Modeling

The WCPS used two mesoscale atmospheric models: the Fifth-Generation Penn State/NCAR Mesoscale Model (MM5: Grell et al. 1995) and the Regional Atmospheric Modeling System (RAMS: Pielke et al. 1992). For both MM5 and RAMS, 48 km resolution simulations of the continental U.S. and portions of the Pacific and Atlantic Oceans were generated. Nested 12 km

grid resolution simulations focused on the high plains, east of the Rocky Mountains to the eastern mid-west, and the 4 km grid resolution simulation were focused on the ARM/CART domain.

4.1.1. An evaluation of MM5-simulated and WSR-88D Radar-derived Precipitation

An evaluation of the precipitation simulated by MM5 using rain-gauge-corrected rainfall estimates from the National Weather Service WSR-88D radar was performed for the ARM/CART domain and the WRW domain for March 2000 (Miller et al. 2003). Modeled and measured precipitation was compared to MM5 simulations at three resolutions, 4 km, 12 km, and 48 km to determine the impact of scale on the model's ability to predict precipitation.

The regional WSR-88D rain gauge-calibrated radar precipitation was provided by the National Weather Service's Arkansas Red River Forecast Center. To evaluate the quality of the radar estimates, the rainfall measurements from March 2000 were compared to independent measurements collected using the high-resolution ABLE rain gauge network in the WRW (11 gauges). Comparisons were made by matching the nearest ABLE rain gauge measurement with the nearest radar estimate in non-convective conditions (Fig. 7). Two days were excluded from the analysis due to obvious convection. For the 27-days that were non-convective, the total accumulated precipitation for the radar and rain gauge estimates was ~56 mm and the two techniques differed in their measurements by 10 mm/day (Fig. 7). Hence, this point-to-point comparison suggests that the two techniques agree to within 20% in non-convective situations. This result is somewhat expected in light of recent studies showing the vulnerability of radar-based precipitation estimates to the spatial variability of precipitation within the measurement volume (Miriovsky et al., 2004) and many past studies that demonstrate other susceptibilities, including

precipitation phase and beam-filling. It is assumed that the radar-based estimates for the entire ARM/CART domain have similar differences.

Figure 7 HERE

MM5 was initialized and updated with NCEP/NCAR Reanalysis II data, and the simulated cumulative 6-hour precipitation was archived for March 2000 for the three different model resolutions. Radar-based rainfall estimates within each MM5 48-km and 12-km grid cell were averaged to produce a rainfall estimate that could be directly compared with the MM5 simulated rainfall. The radar-based rainfall estimates had a typical resolution of 4-6 km over the ARM/CART domain and approximately 5 km over the WRW domain, so no averaging was used for the 4 km comparison.

The MM5 6-hour rainfall estimates over the WRW using 4 km resolution simulations, excluding the two days with obvious convection, show that MM5 underestimates precipitation by 60%, assuming the radar estimates to be accurate to within 20% (Fig. 8a). Although one event (day 3) seems to show a phase lag between onset of precipitation in MM5 and observed precipitation, in general, the timing of precipitation events seems to be well represented by the model when it is run at 4 km resolution. The model has good skill at predicting the occurrence of precipitation, though it has less skill predicting the amount of precipitation that was actually observed. Considering the entire ARM/CART domain (Fig. 8b), improves overall agreement, but MM5 still underestimates precipitation by 37% for the month.

Figure 8. HERE

Similar comparisons for the 12 km and 48 km simulations demonstrate that the agreement between modeled and measured precipitation is scale dependent for March 2000 (Table 3). As discussed above, the MM5 6-hour forecast tends to underestimate the amount of precipitation that was actually observed at a 4 km resolution, regardless of the size of the domain used in the comparison. In contrast, the 12 km resolution MM5 shows good skill at forecasting the total amount of observed precipitation. At 48 km, the size of the comparison domain becomes an important issue; the precipitation in the WRW is significantly underestimated, while that over the ARM/CART domain is well represented.

The variability in the radar-observed and MM5 simulated precipitation is also scale dependent. At 4 km, MM5 faithfully represents the observed variability in precipitation from point-to-point., while at 12 km resolution, the model, particularly in the WRW domain, overestimates variability in observed precipitation.

These results suggest that MM5 simulations of non-convective rainfall over the WRW and the ARM ACRF site, which is approximately the size of a global climate model grid cell, are sensitive to the selected horizontal resolution, at least during the month that was analyzed here. This sensitivity should be analyzed in more detail in future studies and should be considered when using MM5 to simulate hydrologic processes, either as an independent entity, or as a future parameterization in a global climate model (Randall et al., 2003). It is difficult to make a credible attempt to evaluate the required accuracy of precipitation estimates because it is both application dependent and integrally linked to other processes within the hydrologic system (i.e. evapotranspiration).

Table 3. HERE

4.1.2.. Implementation of Water Isotopes Modeling in MM5

An important tool for testing the moisture process parameterizations in mesoscale models is to track stable water isotopes. Because the physical processes that alter isotopic ratios are well known, they can be used a benchmarks when simulated isotopic ratios are compared to observations. A stable isotope routine is being developed for MM5 (Foster et al. 2003). While a number of global climate models (GCMs) have isotope tracing routines (Noone & Simmonds 2002, Jouzel 1987), this will be one of the first regional climate models with such a scheme. A major obstacle to evaluating a regional isotope model is the lack of a dense network of isotopic measurements. The intensive observations and modeling carried out via the WCPS offers an opportunity to locally evaluate isotopic predictions of the regional climate model. As with the modeled rainfall versus radar, as well as the modeled vegetation cover versus satellite imagery, stable isotope simulations are being tested at several spatial scales. At the largest grid, 48 km, the United States and parts of the Pacific and Atlantic Oceans are simulated. At this scale, tests for the observed trend of decreasing isotopic values along inland heading transects, including from southern Texas to Oklahoma, using the data sampled from the NADP network. Since GCMs can capture similar latitudinal gradients (Jouzel et al. 1987), we expect the MM5/Isotope model to be able to capture this signal. We will also examine the observed increase the d-excess observed in Oklahoma relative to Texas. The nested grid with a 12 km resolution will be tested against the seasonal source signal in the isotopic values seen in Oklahoma. And finally, we are attempting to use the nested 4 km resolution simulations to reproduce the isotopic values of the atmospheric vapor samples collected over the WRW domain. Work has been initiated to reproduce the decreasing isotopic ratios observed in the 22-26 May 2002 convective events that were part of the IOP. Should these tests prove successful, we will be able to determine the sources of the local water, and to what extent it is advected into the region and locally re-evaporated. The value of the

d-excess has long been used as a proxy for the source of water and this model will allow us to test this hypothesis on a small scale. This sub-study is not yet complete, and forthcoming results will be reported elsewhere.

4.1.3. Fine Scale Sensitivity Simulations using RAMS

Another critical issue with the use of mesoscale models is the relationship between the models' vertical resolution and the amount and distribution of precipitation that it produces. Relatively fine vertical grid spacing can allow for better resolution of the vertical structure of the moisture and wind fields, but leads to higher computational cost. Simulations were generated with the four-nested grid configuration of RAMS employing two different vertical resolutions near the surface, and the precipitation results were compared as a test of the model's sensitivity to vertical resolution. The simulation with the finer vertical resolution used 50 m vertical grid spacing near the surface and a total of 46 vertical levels. At heights of 300 m above ground level (AGL), the grid spacing was gradually increased to 750 m. In the coarser vertical resolution case, the vertical grid spacing began at 200 m and increased above 400 m AGL to 750 m. In this run, 35 vertical levels were used. In both cases, the model top extended above 20 km.

Model predictions of the precipitation event on 2-3 March 2000 were compared between the two runs. Precipitation in the WRW began in the southern and western sections, with the Oxford precipitation gage (Fig. 2) initially recording measurable amounts at about 1330 UTC on 2 March. The rain then spread to the east and north, ending in the WRW by roughly 1100 UTC on 3 March. RAMS predictions also indicate that the precipitation started in the southern and western sections of the watershed; however, both of the RAMS simulations tend to initiate the precipitation a couple

of hours later than observed and precipitation totals for the event were under-predicted, particularly at the two most northern rain gauge stations, Whitewater and Beaumont.

Comparing the two simulations with different vertical resolution shows that precipitation totals were similar in the southern half of the watershed. In the RAMS simulation with 50 m vertical grid spacing near the surface, the precipitation pattern moves to the east with little rain spreading to the northern sections of the watershed. The simulation with 200 m vertical resolution produces a rainfall pattern that spreads to the east and north and precipitation totals at the Whitewater and Beaumont locations are closer to, although still somewhat less than, observed. Figure 9 presents the rainfall rates at 0000 UTC on 3 March 2000, as predicted by the two RAMS simulations. While the amounts are similar, the coarser vertical resolution places the greatest amounts further north, which leads to the greater precipitation predictions at the Whitewater and Beaumont sites.

Thus, for this single, non-convective, synoptically driven case, finer vertical grid spacing near the surface does not dramatically affect precipitation totals estimated by the model. However, it does affect the horizontal distribution of the modeled precipitation within the WRW. In this case, the horizontal distribution is in better agreement with observations when the coarser vertical resolution is used. The results will likely be different for other cases, particularly where near surface features, such as a low-level jet, play an important role, but higher computational costs can be avoided using coarser vertical resolution.

Figure 9. HERE

4.2. Land Surface Hydrologic Modeling The treatment of the land-surface is an essential element of water cycle modeling. In this section, model results from two schemes are discussed.

4.2.1. Scale Analysis Using the TOPmodel-based Land Atmosphere Transfer Scheme: TOPLATS

The land surface hydrologic model used here for evaluating scale dependent processes is the TOPMODEL-based Land-Atmosphere Transfer Scheme, TOPLATS (Famiglietti and Wood 1994). For this study, TOPLATS was set up and calibrated in several modes, including a fully distributed 30 m resolution mode, a 30 m combined statistical-distributed mode (1 km probability distributions based on 30 m resolution data), a 1 km resolution fully-distributed mode, and a single column mode. Several variations of these modes were calculated using uniform or distributed input forcing and characterizations. In the absence of fine scale spatial observations, the 30 m resolution fully distributed mode was used as a baseline for relative comparison of model performance. Simulations were for 1 January 1999 to 31 December 2000 for all modes, except the 30 m fully distributed mode, which was limited to 14 July to 22 September 2000 due to computational demands. TOPLATS verification based on comparison of the 1 km distributed model runoff data and the observed streamflow data at the Towanda gauge had fair to good agreement, with a Nash Efficiency of 0.65. TOPLATS modes were compared for the common 14 July to 22 September 2000 time period.

Eleven simulations were performed with different modes, and with several variations in the representations of spatial variability of precipitation, land use, topography, and soils to assess the sensitivity of the model response (Table 4). Hourly precipitation was prescribed as uniform over the watershed or at 1 km resolution. The land use and vegetation types were represented as uniform over the watershed, at 1 km or 30 m resolutions, or 1 km distributions based on 30 m data. Using

30 m DEM data, topography index (the tangent of the ratio of the upstream flow area through a grid cell to the slope of the cell) distributions for the WW were determined. These represented the topography as uniform at 1 km resolution, and non-uniform at 1 km and 30 m for the whole catchment. Finally, the soil types were represented at 1 km resolution or uniform over the watershed.

Model results suggest that in parts of the catchment evapotranspiration switched between being atmospherically controlled to soil moisture controlled after 19 July. Comparison between the TOPLATS modes (Fig. 10) indicates that the combined distributed-statistical approach and the 30 m fully distributed mode, both evaluated at a 1 km resolution resulted in near identical water and energy fluxes, soil moisture, and runoff values. The statistical-distributed mode is significantly less computationally demanding and has far fewer parameters. The fully distributed 1 km resolution of TOPLATS led to an underestimate of runoff and an overestimate of evapotranspiration. The statistical mode resulted in an overestimate of runoff, and the column mode gave no runoff and had an extreme overestimate of evapotranspiration. Results of this study are summarized in Tables 4a and b.

This study provides insight into how spatial variability can be represented without using a fully distributed model at fine-scale. The similarity between the spatially averaged data from the distributed-statistical and the fully distributed simulations suggests that the distributed-statistical mode is an effective way of reducing computer resources required while reproducing vertical fluxes. Lateral transport remains dependent on local information carried via a fully–distributed mode.

Table 4. Here

Figure 10. HERE

4.2.2. PArameterization of Subgrid-scale Surface (PASS) Model

It is important for regional surface modeling to have accurate descriptions of sub-grid and seasonal variations in surface fluxes, or biases may be introduced. To address this and to aid in the study of the interannual variability of key surface hydrological components, the Parameterization of Subgrid Scale (PASS) model (Song et al. 2000a, b) focused on a five-year simulation (1996-2000) at the WRW. This study ties in with the TOPLATS study by providing a finer scale with a longer simulation period. Long multi-year simulations and analyses with the fully distributed 30 m resolution version of TOPLATS were not computationally feasible within the constraints of this pilot project.

The PASS model simulates land surface processes at sub-grid scales up to 1 km and higher using a fairly simple approach to simulate evapotranspiration and root-zone available soil moisture (RAM). It is based in part on AVHRR-derived NDVI data and conventional surface meteorological data. Biweekly composite 1 km resolution NDVI values processed by the USGS were adjusted to compensate for atmospheric effects producing surface estimates of NDVI. The spatial NDVI variability is large and occurs on scales smaller than 1 km. Long-term simulation of evapotranspiration using PASS requires continuous biweekly data on surface conditions.

The five-year input data set was constructed from meteorological observations at the WRW and the ARM/CART extended facility near Towanda, Kansas. WRW surface precipitation consisted of 4 km resolution Nexrad data adjusted with rain gauge observations supplied by the Arkansas-Red Basin River Forecast Center. Daily streamflow data at Winfield, Kansas (Fig. 2)

were obtained from the USGS and compared to PASS runoff estimates, which were derived as the residual term in the water balance.

The initial RAM value for all pixels was assumed to be the maximum value, that is, the available moisture capacity for the dominant soil type in each pixel, and surface runoff was assumed to occur when the estimated RAM exceeded this value. This water excess was assumed to be lost from soil layers contributing to evapotranspiration, but the additions to local streamflow and groundwater recharge were not estimated in this simple model. Total runoff was assumed to be the difference between precipitation and evapotranspiration if the RAM for the entire WRW is the same at the end of the computational period as it was at the beginning and water losses through the bedrock were negligible. Also, the amount of time for the water balance computations should be sufficiently long to relegate changes in soil and groundwater storage to small contributions relative to the precipitation and evaporation. Fig. 11 shows the result for this method of runoff calculation, relative to the streamflow at Winfield stream gauge station. The average RAM calculated for the WRW is lowest in the late summer, when rainfall is limited and evaporative demand is high, and is highest in the winter. Except for the transition between 1997 and 1998, this soil moisture storage appears to be consistently at very large values at the end of the yearly computational periods.

Figure 11. HERE

Over the five-year period, the modeled water loss from evapotranspiration accounts for 70-90% of precipitation at the end of each year, which is reasonable for southern Kansas. The differences between the observed streamflow and modeled runoff are less than 25% and seem to depend on the precipitation amount and distributions. For example, the differences are smaller for

1996 and 2000, when precipitation was spread evenly across the year, than for 1998 and 1999, when large precipitation events occurred rather late in the year. Relatively large evapotranspiration rates beginning in the summer of 1997 led to the lower RAM at the end of the year, and the resulting deficit in the soil moisture in early 1998 led to reduced runoff until a large precipitation event occurred in October. Rather large evapotranspiration rates were also simulated for the summer of 1999, mostly driven by high precipitation rates that increased RAM. Overall, the modeled runoff is less than or equal to observed streamflow, suggesting that modeled evapotranspiration estimates might be too large. It is suspected that when the rain rate is high, more runoff occurs as a result of a limited infiltration rate. This process will be considered in the next set of PASS model improvements.

To allow examination of some of the details of evapotranspiration, modeled and observed daily means of latent heat fluxes at WW are plotted (Fig. 12). While the variations appear to be well captured, the best-fit line is slightly steeper than the 1:1 line, indicating some model overestimation.. Large spatial variation exists even for five-year total accumulated values (Fig. 13). The pattern of higher evapotranspiration corresponds to higher-precipitation pixels except in the southern part of the WRW, where an east-west belt of higher precipitation corresponds to higher runoff. Several strong precipitation events had occurred along this east-west belt in the southern WRW. On average, evaporative water loss accounts for nearly 80% of precipitation, and runoff accounts for 20%.

Figure 12. HERE

Figure 13. HERE

Preliminary results indicate that accumulative surface evapotranspiration was slightly overestimated, which resulted in underestimates of cumulative runoff within the WRW as compared to observed streamflow at the outlet of the WRW; the maximum yearly underestimate was 25%, in year 1998. Diurnal and seasonal changes in modeled evapotranspiration in year 2000 matched fairly well with the in situ flux measurements despite a slight overestimation in cumulative evaporative water loss during certain periods at certain sites. These results suggest that a highly parameterized is of value, but PASS can be improved to efficiently estimate long-term surface hydrological components. It is expected that continued work on selection of proper root-zone depths for various types of vegetation and on runoff process treatment will improve the water budget.

5. Summary and Recommendations

The WCPS study represents an organized effort to pool many sources of hydrologic data to provide a framework for evaluating the hydrologic cycle via regional models and to better understand the requirements for linking such regional processes to climatic scale forces that modulate the water cycle. It was centered on the use of observations and modeling toward closing the water budget of a small, representative watershed, and understanding the links between large- and local- scale processes that modulate the water budget.

Primary findings based on the two research questions addressing water budget closure are summarized below:

The latent heat flux shows large variability at small scales (<1 km) and is sensitive to the spatial distribution of vegetation, soil moisture, access of deep-rooted plants to groundwater, and

local atmospheric processes. While considerable information about the surface characteristics can be gained from satellite retrievals, sufficient *in situ* measurements to evaluate these retrievals and existing parameterizations (e.g. TOPLATS and PASS) are seriously lacking. Achieving true closure of the water budget of the WRW will require a long-term, coordinated measurement campaign to quantify components of the latent heat flux and measurement uncertainty.

Soil moisture and deeper groundwater measurements are scarce in the WRW. Soil moisture varies considerably on scales of only a few meters, and a detailed and coordinated measurement campaign to would be required to properly quantify these variations. To achieve observational closure, it would be necessary to sample soil moisture regularly and with sufficient resolution to resolve the largest sources of variance (100 m or less). While satellite measurements may provide a gross measure of soil moisture, they do not have sufficient resolution to achieve the process-level understanding that is required to evaluate model representations. Deeper groundwater is expensive to measure and was grossly under-sampled during the WCPS, mostly due to cost. Observational closure in the WRW would require a sampling strategy that is linked to the geological structure of the region and a coordinated measurement strategy.

There is a wealth of precipitation data available for the WRW. Notwithstanding, there remains considerable uncertainty in the radar-based measurement of precipitation, although polarized radar is known to provide better estimates. Simulations with MM5 and RAMS suggest that the precipitation parameterizations used in the models are sensitive to vertical and horizontal resolution. The WCPS suggests that a concerted effort to measure and model precipitation in the WRW would involve the long-term use of polarized radar, a dense network of independent rain gauges (gauges not used in the radar precipitation algorithm), and a comprehensive study of model performance over many seasons.

Observational closure of the water budget in the WRW would require systematic measurement of stream flow at all exit branches, rather than measurements designed primarily for flood forecasting. Reservoir levels would also have to be measured, along with the water levels in larger farm ponds.

Long term monitoring of isotopic fractionations in the WRW would provide the necessary links to the climate system and a pathway for examining feedbacks within the system. Isotopic monitoring of runoff, precipitation, and groundwater combined with model simulations of isotopic fractionations would provide a medium for understanding shortfalls in the models and provide a key element in water cycle prediction by linking specific conditions within the watershed with the large scale transport of water from sources.

Acknowledgements:

This work was supported by the U.S. Department of Energy, Office of Science, Office of Biological under contract DE-AC03-76F00098 for LBNL, contract DE-AC05-00OR22725 for ORNL, contract DE-AC02-98CH10886 for BNL, contract W-7405-ENG-36 for Los Alamos, and contract W-31-109-Eng-38 for ANL. Individuals who contributed to this study include Susan Kemball-Cook and Don DePaolo at LBNL, Tracy Schofield and Peter Beeson at LANL, and David Cook, Donna Holdridge, Richard Coulter, and Timothy Martin at ANL, Vonekia Atkinson, Selena Mellon, and Mike Sale at ORNL. This manuscript is LBNL Report LBNL-53826.

The DOE Water Cycle Pilot Study is dedicated to the memory of Dr. Marvin L. Wesely.

References

Aber, J.D, R.C. Bales, J. Bahr, K. Beven, E. Foufoula-Georgiou, G.M. Hornberger, G. Katul, Kinter, R. Koster, D. Lettenmaier, D. McKnight, K. Miller, K. Mitchell, J. Roads, B.R. Scanlon, E. Smith, 1999: Global Water Cycle Initiative, 81 pp.

Baldocchi, D.D., 2003: Assessing the eddy covariance technique for evaluating carbon dioxide rates of ecosystems: past, present and future. *Global Change Biology*, **9**, 479-492.

Bashford KE., K.J. Beven, and P.C. Young, 2002: Observational data and scale-dependent parameterizations: explorations using a virtual hydrological reality, Hydro Process, **16**, 293-312.

Bashford, K.E., H. Shariff, W.T. Crow, N.L. Miller, and E.F. Wood, 2003: An investigation of scale and variability using fully- and semi-distributed TOPLATS at the Whitewater watershed, Kansas, 83rd AMS Meet., 9-13 February 2003, Long Beach, CA., 162-163.

Beven, K.J, R. Lamb, P.F. Quinn, R. Romanowicz, and J. Freer 1995: TOPMODEL. In Singh (Ed.), Computer Models of Watershed Hydrology. Water Res. Publ., Highland, Colo. 627-668.

Chen, F. and J. Dudhia, 2001: Coupling an advanced land-surface/hydrology model with the Penn State/NCAR MM5 modeling system. Part I: Model implementation and sensitivity. *Mon. Wea. Rev.*, 129, 569-585.

Crow, W.T. and E.F. Wood, 2002: The value of coarse-scale soil moisture observations for regional surface energy balance modeling. *J. Hydrometeor*., **3**, 467-482.

Department of Energy, 2002: The Water Cycle Research Strategy, DOE SC-0043, Office of Biological and Environmental Research, Germantown, MD. May 2002.

Famiglietti, J.S. and E.F. Wood, 1994: Multi-scale modeling of spatially variable water and energy balance processes. *Water Resour. Res.*, **30**, 3061-3078.

Foster, P.N., N.L. Miller, and D.J. DePaolo, 2003: Implementation and testing of water isotopes into a regional climate model. IAHS, IUGG, Sapporo, Japan, 30 June to 11 July 2003, B.360.

Gibbs, H.K., A.W. King, R.A. Washington-Allen, F. Pan, and M. Sale. 2003: The Walnut River Watershed Geographic Information System at ftp.esd.ornl.gov (cd /pub/pilot_study) Oak Ridge National Laboratory, Oak Ridge, Tennessee, U.S.A.

Grell, G., 1993: Prognostic evaluation of assumptions used by cumulus parameterizations. *Mon. Wea. Rev.*, **121**, 764-787.

Grell, G.A., J. Dudhia, and D.R. Stauffer, 1995: A description of the Fifth-Generation Penn State/NCAR Mesoscale Model (MM5). NCAR/TN-398+STR, 117pp.

Henderson-Sellers, A., Z-L Yang, and R.E. Dickinson, 1993: The project for intercomparison of land surface schemes. *Bulletin of the Amer. Meteor. Assoc*., **74**, 1335-1349.

Hong, S.-Y, and H.-L. Pan, 1996: Nonlocal boundary layer vertical diffusion in a medium-range forecast model. *Mon. Wea. Rev.*, **124**, 2322-2339.

Hupet, F. and M. Vanclooster. 2002. Intraseasonal dynamics of soil moisture variability within a small agricultural maize cropped field. *J. Hydrology*, **261**, 86-101.

Jouzel, J., Russell, G.L., Suozzo, R.J., Koster, R.D, White, J.W.C. and W.S. Broecker 1987, Simulations of the HDO and H218O Atmospheric cycles using the NASA GISS general circulation Model: The seasonal cycle for present-day conditions", *J. Geophys. Res*., **92**, 14739-14760.

Kansas Water Office 1997. http://www.kwo.org/Org_People/walnut.htm

Lawford, R.G., 2001: Integration of land observations and modeling: Experiences and strategies of a large scale experiment. *In Land Surface Hydrology, Meteorology, and Climate: Observations and Modeling.* Ed. V. Lakshmi, J. Albertson, J. Schaake, Water Sci. and App. **3**, 215-230.

Lawford, R.G., 1999: A midterm report on the GEWEX Continental-scale International Project (GCIP). *J. Geophys. Res*., **104**, 19279-19292.

LeMone, M.A., R.L. Grossman, R.L. Coulter, M.L. Wesely, G.E. Klazura, G.S. Poulos, W. Blumen, J.K. Lundquist, R.H. Cuenca, S.F. Kelly, E.A. Brandes, S.P. Oncley, R.T. McMillen, and B.B. Hicks, 2000: Land-atmosphere interaction research, early results, and opportunities in the Walnut River Watershed in southeast Kansas: CASES and ABLE. *Bull. Amer. Meteor. Soc*., **81**, 757-779.

Lohmann, D., D.P. Lettenmaier, X. Liang, E.F. Wood, and others, 1998: The Project for Intercomparison of Land Surface Schemes (PILPS): Phase 2C, Red-Arkansas River Basin experiment, 3, Spatial and temporal analysis of water fluxes. *Global and Planetary Change*, **19**, 161-176.

Machavaram, M.V., M.E. Conrad, and N.L. Miller, 2003: Precipitation induced variations in streamflow. 83rd AMS Meet., 9-13 February 2003, Long Beach, CA., 204. *Manuscript in Review.*

Mahrt, L. and H-L Pan, 1984: A two-layer model of soil hydrology. Bound Layer Met., **29**, 1 – 20.

Miller, M.A., D.T. Troyan, N.L. Miller, J. Jin, S. Kemball-Cook, and K.R. Costigan, 2003: Water cycle variability over a small watershed: A one month comparison of measured and modeled precipitation over the Southern Great Plains. , 83rd AMS Meet., 9-13 February 2003, Long Beach, CA., 9-10. *Manuscript in Preparation.*

Miriovsky,B.J., Allen, B. A. Eichinger,W.E., Krajewski,W.F., Kruger,A., Nelson,B.R., Creutin,J., Lapetite,J., Lee,G.W., Zawadzki,I., Ogden,F. L., 2004: An Experimental Study of Small-Scale Variability of Radar Reflectivity Using Disdrometer Observations

J. Appl. Met., **43**: 106-118

Noone D. and I. Simmonds, 2002: Associations between delta O-18 of water and climate parameters in a simulation of atmospheric circulation for 1979-95. *J. Climate*, **15**, 3150-3169.

NRC (National Research Council). 2002. Review of the USGCRP plan for a new science initiative on the global water cycle. *National Academy Press*, Washington, D. C., 44pp.

Pielke, R.A., W.R. Cotton, R.L. Walko, C.J. Tremback, M.E. Nicholls, M.D. Moran, D.A. Wesley, T.J. Lee, and J.H. Copeland, 1992: A comprehensive meteorological modeling system - RAMS. *Meteor. Atmos. Phys.*, **49**, 69-91.

Song, J., M. L. Wesely, R. L. Coulter, and E. A. Brandes, 2000a: Estimating watershed evapotranspiration with PASS. Part I: Inferring root-zone moisture conditions using satellite data, *J. Hydrometeor*., **1**, 447-461.

Song, J., M. L. Wesely, M. A., LeMone, and R. L. Grossman, 2000b: Estimating watershed evapotranspiration with PASS. Part II: Moisture budget during drydown periods, *J. Hydrometeor*., **1**, 462-473.

Takle, E.S., W.J. Gutowski, R.W. Arritt, Z.T. Pan, C.J. Anderson, R.R. da Silva, and others, 1999: Project to Intercompare Regional Climate Simulations (PIRCS): Description and initial results. *J Geophys. Research*, **104**, 19443-19461.

Tremback, C.J., 1990: Numerical simulation of a mesoscale convective complex: model development and numerical results. Ph.D. dissertation, Atmos. Sci. Paper No. 465, Department of Atmospheric Science, Colorado State University, Fort Collins, CO 80523, 247 pp.

Walko, R.L., L.E. Band, J. Baron, T.G.F. Kittel, R. Lammers, T.J. Lee, D. Ojima, R.A. Pielke, C. Taylor, C. Tague, C.J. Tremback, and P.L. Vidale, 2000: Coupled Atmosphere-biosphere-hydrology models for environmental modeling. *J. Appl. Meteor*., **39**, 931-944.

Walko, R.L., W.R. Cotton, M.P. Meyers, and J.Y. Harrington, 1995: New RAMS cloud microphysics parameterization. Part I: The single-moment scheme. *Atmos. Res*., **38**, 29-62.

Welles, J. M. 1990. Some indirect methods of estimating canopy structure, In: N.S. Goel and J.M. Norman. (eds.) Instrumentation for studying vegetation canopies for remote sensing in optical and thermal infrared regions. *Remote Sensing Rev*, **5**, 31-43.

Wood, E.F., D.P. Lettenmaier, X. Liang, D. Lohmann, and others, 1998: The Project for Intercomparison of Land Surface Schemes (PILPS): Phase 2C, Red-Arkansas River Basin experiment, 1, Experimental description and summary intercomparisons. *Global and PLanetaary Change*, **19**, 115-135.

Wood, E.F., 1994: Scaling, soil moisture, and evapotransipartion in runoff models. *Advances Water Res*., **17**, 25-34.

Wood, E.F., M. Sivapalan, K. Beven, and L. Band, 1988: Effects of spatial variability and scale with implications to hydrologic modeling. *J. Hydrology*, **102**, 29-47.

Table Captions

Table 1 The set of WCPS tasks, what was done, and who did are provided.

Table 2. Within-vegetation type spatial variability in predicted LAI for Whitewater Watershed. The minimum is defined by the 10th percentile and the maximum by the 90th percentile of the distribution of LAI values within a vegetation type.

Table 3. Ratios of means and standard deviations between radar-measured and modeled precipitation over the Walnut River Watershed (WRW) and the entire ARM/CART site**.**

Table 4 a) Model experiment, description, and resolution. RMSE refers to root mean squared error relative to the baseline case. b) Resulting net flux, latent heat, sensible heat, and ground heat for each model experiment, c) Evapotranspiration (ET), surface and subsurface runoff, water table depth, and percent soil moisture (upper and lower) for each model experiment.

Figure Captions

Figure 1. A. The ARM/CART Southern Great Plains Site, and B. the Walnut River Watershed with existing measurements.

Figure 2. Spatial distribution of LAI in the Whitewater Watershed simulated by applying empirical LAI-NDVI relationships to 30m Landsat-TM NDVI data collected in July 2002.

Figure 3. TOPLATS' simulated latent heat flux for different vegetation types in the Whitewater Watershed assuming different values of LAI. See Table 2 for LAI values.

Fig. 4. Hourly water surface elevations for well A272 (A), a shallow saturated zone, well B295 (B), a deeper saturated zone, and a Potwin supply well (C).

Figure 5. Soil water contents from Rock Creek hillslope for the period 5-7 June 2002 measured with portable time-domain reflectometry system.

Figure 6. A) Precipitation amounts at the APO, B) $\delta^{18}O$ concentration in precipitation at the APO, C) $\delta^{18}O$ concentration in rivers at the Walnut River, Whitewater River, and at the junction of the Walnut and Whitewater Rivers.

Figure 7. Results from two independent rainfall estimates over the WRW using the HRAP 4 km data.

Figure 8. MM5-simulated 4 km precipitation and WSR-88D Radar-derived precipitation during March 2000 for A) WRW domain and B) the ARM/CART domain.

Figure 9. The rainfall rates at 0000 UTC on 3 March 2000, as predicted by the RAMS simulations with 35 vertical levels and 46 vertical levels.

Figure 10. Comparison of the 30m Distributed, Combined Statistical-Distributed, 1km Distributed, and Single Colum for A) Evapotranspiration on 24 July, B) Evapotranspiration on 13 September, C) Surface Runoff for 17 July and D) Surface Runoff for 28 July 2000.

Figure 11. Modeled and observed yearly accumulative values of surface hydrological components at the WRW and modeled root-zone available moisture during 1996-2000.

Fig. 12. Comparison of modeled versus observed daily mean latent heat fluxes in year 2000 at the Whitewater site. The solid line represents a linear regression fit.

FIG. 13. Total modeled evapotranspiration (left), total modeled runoff (center), and observed precipitation (right) for the WRW during 1996-2000.

Tasks	What	Who
Data Analysis	JJA and DJF; Storm Events	
Archived Climate Data	WRW streamflow and precipitation, radar-based microphysics @ CF, WRW baseline analysis	BNL ANL
Archived Isotope Data	Obtain available water isotope rain gauge, streamguage, flux data	LBNL
Archived Surface Data	Weather variables, LAI	ORNL, ANL
Modeling		
Atmospheric	36 and 12 km resolution add water isotope mass conservation equations 1 km resolution	 LBNL LANL
Land Surface	Water, energy, momentum fluxes	All
Hydrology	Fully Distributed with groundwater 100m resolution Spatially distributed 50 m resolution with ($\delta^{18}O$,δD) and validation	LANL LBNL
Isotopes		
Isotope Sampling	3-6 Precip,1 streamflow, 3Flux, soil water	LBNL, ANL
Isotope Analysis	Analysis of $\delta^{18}O$, δD	LBNL
Validation	Model and Observation Comparison	All

Table 1. The set of WCPS tasks, what was done, and who did are provided.

Vegetation	Mean	Minimum	Maximum
Grassland	2.08	0.43	3.73
Row Crop	2.11	0.46	3.78
Woodland	2.17	0.60	3.77

Table 2. Within-vegetation type spatial variability in predicted LAI for Whitewater Watershed. The minimum is defined by the 10th percentile and the maximum by the 90th percentile of the distribution of LAI values within a vegetation type.

	μ (Radar)/ μ (MM5) [σ(Radar)/ σ(MM5)]		
	4-km	12-km	48-km
WRW	1.68 [1.10]	1.07 [0.68]	1.32 [0.92]
CART	1.41 [1.14]	1.11 [0.84]	1.01 [0.83]

Table 3. Ratios of means and standard deviations between radar-measured and modeled precipitation over the Walnut River Watershed (WRW) and the entire ARM/CART site**.**

	Net flux		Latent		Sensible		Ground	
	(W/m^2)		(W/m^2)		(W/m^2)		(W/m^2)	
	Mean	RMSE	Mean	RMSE	Mean	RMSE	Mean	RMSE
BLFD30m	186.97	0.00	86.38	0.00	95.36	0.00	5.23	0.00
COMB	186.76	0.75	85.60	4.44	96.03	3.21	5.14	1.33
COMBpws	186.92	0.77	86.31	5.46	95.13	3.45	5.49	2.33
COMBtop1km	190.40	3.80	95.89	15.17	89.48	11.07	5.04	4.57
STAT	187.18	1.07	88.48	7.73	93.18	5.56	5.53	2.93
STATnotop	187.31	1.37	89.59	10.52	92.32	8.86	5.42	4.94
DIST1km	190.17	3.46	93.90	13.00	91.22	8.70	5.06	3.68
COL	196.37	9.76	97.25	22.80	94.31	14.60	4.81	12.03

	Evapotranspiration		Surface Runoff		Subsurface Runoff	
	(mm)		(mm)		(mm)	
	Mean	RMSE	Mean	RMSE	Mean	RMSE
BLFD30m	0.128	000	9.232e-03	000	2.605e-04	000
COMB	0.127	6.548e-03	9.486e-03	2.040e-03	2.589e-04	1.990e-06
COMBpws	0.128	8.063e-03	9.764e-03	9.157e-03	2.582e-04	2.651e-06
COMBtop1km	0.142	2.255e-02	9.023e-03	1.724e-03	2.423e-04	1.865e-05
STAT	0.131	1.142e-02	1.087e-02	2.620e-02	2.300e-03	2.216e-03
STATnotop	0.133	1.559e-02	000	1.149e-01	3.593e-03	3.369e-03
DIST1km	0.140	1.934e-02	4.998e-03	5.396e-02	3.082e-04	5.244e-05
COL	0.145	3.386e-02	000	1.149e-01	3.402e-03	3.179e-03

	Water table depth		Soil Moisture		Soil Moisture	
	(mm)		Upper Zone		Lower Zone	
	Mean	RMSE	Mean	RMSE	Mean	RMSE
BLFD30m	1924	0.00	0.337	0.0000	0.336	0.0000
COMB	1924	0.77	0.337	0.0012	0.337	0.0011
COMBpws	1925	1.25	0.336	0.0025	0.336	0.0004
COMBtop1km	1947	25.86	0.340	0.0052	0.354	0.0186
STAT	1962	39.54	0.340	0.0046	0.342	0.0056
STATnotop	1818	123.49	0.316	0.0224	0.325	0.0208
DIST1km	1870	58.55	0.331	0.0065	0.340	0.0104
COL	1833	108.20	0.314	0.0250	0.315	0.0299

Effect of varying representation of spatial variability on water table depth and soil moisture (catchment average)
[RMSE refers to root mean squared error relative to the baseline case]

Experiment	Description	Resolution
BLFD	Baseline (Distributed)	30m
COMB	Combined (Dist. 1km w/30m index)	1km/30m
COMBpws	Combined, uniform precipitation	1km/30m
STAT	Statistical	30m
STATnotop	Statistical	30m
DIST1km	Distributed	1km
COL	Lumped Column	ws

Table 4 Model experiment, description, and resolution. RMSE refers to root mean squared error relative to the baseline case. a) Resulting net flux, latent heat, sensible heat, and ground heat for each model experiment, b) Evapotranspiration (ET), surface and subsurface runoff, and c) water table depth, and percent soil moisture (upper and lower) for each model experiment. Ws-uniform for watershed.

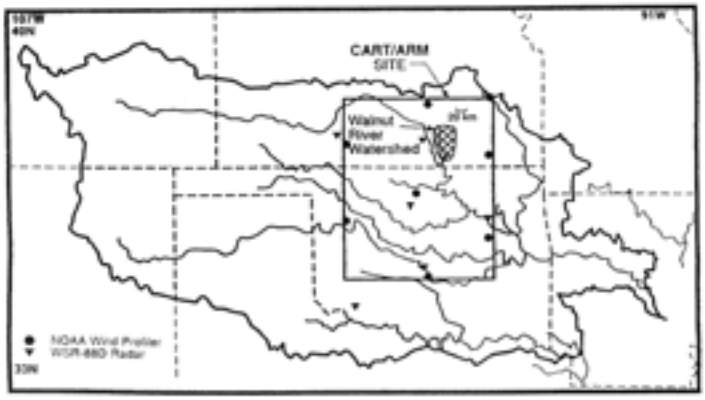

Figure. 1. A). The ARM/CART SouthernGreat Plains Site and B). the nested Walnut River Waters with existing measurements.

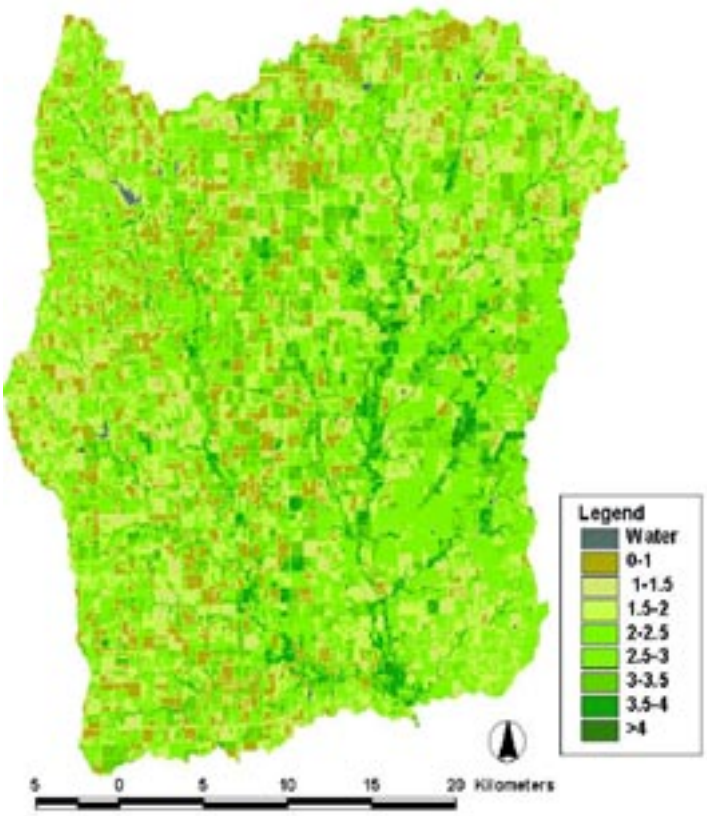

Figure. 2: Spatial distribution of LAI in the Whitewater Watershed generated by applying empirical LAI-NDVI relationships to 30m Landsat-TM NDVI data collected July 2002.

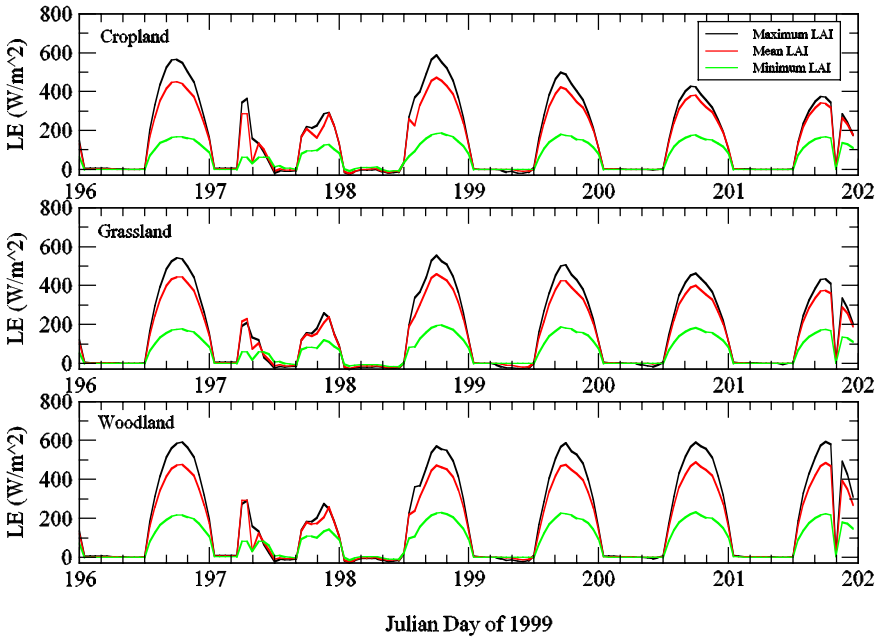

Figure 3. TOPLATS' simulated latent heat flux for different vegetation types in the Whitewater Watershed assuming different values of LAI. See Table 2 for LAI values.

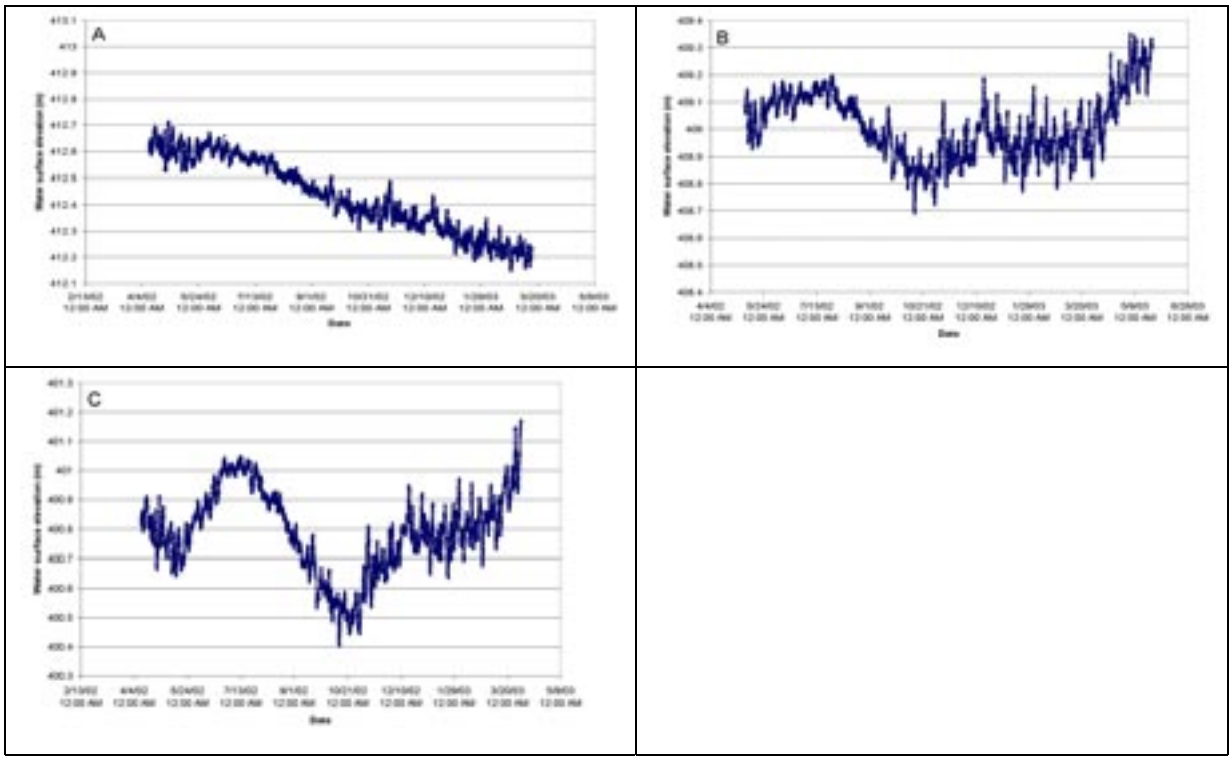

Figure 4. A). Hourly water surface elevations for well A272, B). a shallow saturated zone, well B295 (B), a deeper saturated zone, and C). a Potwin supply well.

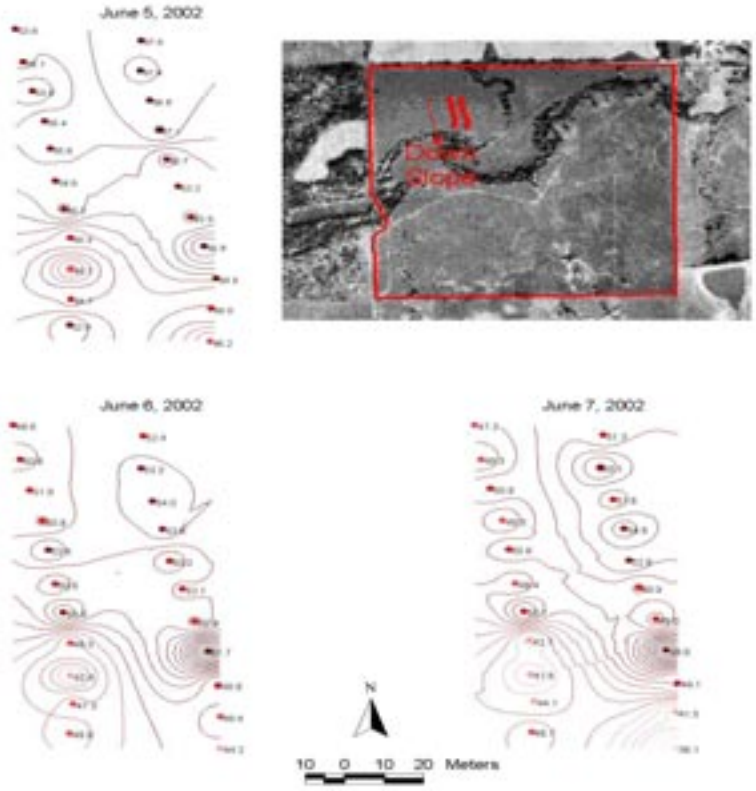

Figure 5. Soil water contents from Rock Creek hillslope for the period 5-7 June 2002 measured with portable time-domain reflectometry system.

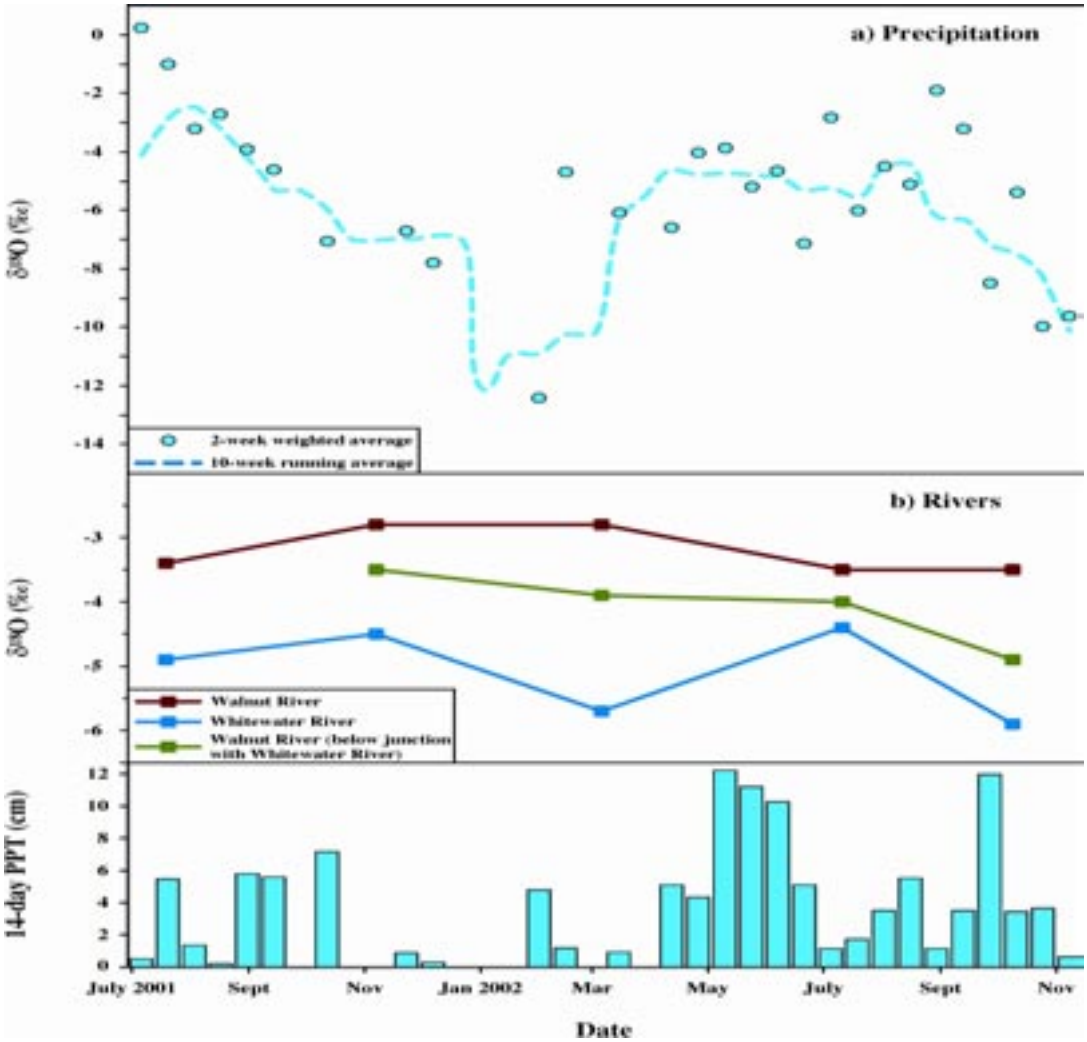

Figure 6. Samples for the period July to November 2001, where A) is the 14-day cumulative precipitation amounts at the ABLE Project Office (APO) site, B) is the 2-week weighted average and 10-week running oxygen isotope concentration in precipitation, and C) is the oxygen isotope concentration in streamflow at Walnut River, Whitewater River, and Walnut River below the Whitewater River junction.

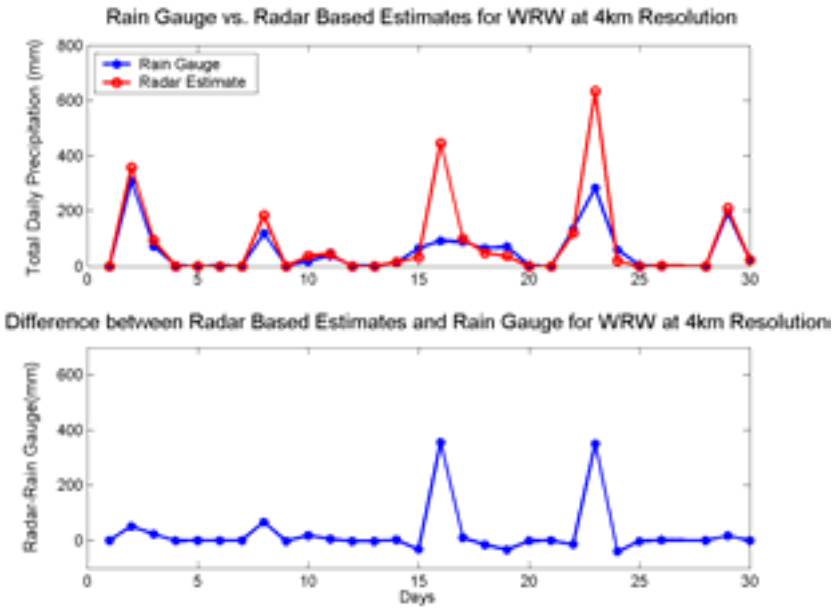

Figure 7: Results from two independent rainfall estimates over the WRW using the 4 km data supplied by the Arkansas Red River Forecast Center. Convective conditions were observed on 16 and 23 March, which accounts for the large discrepancies observed on those days.

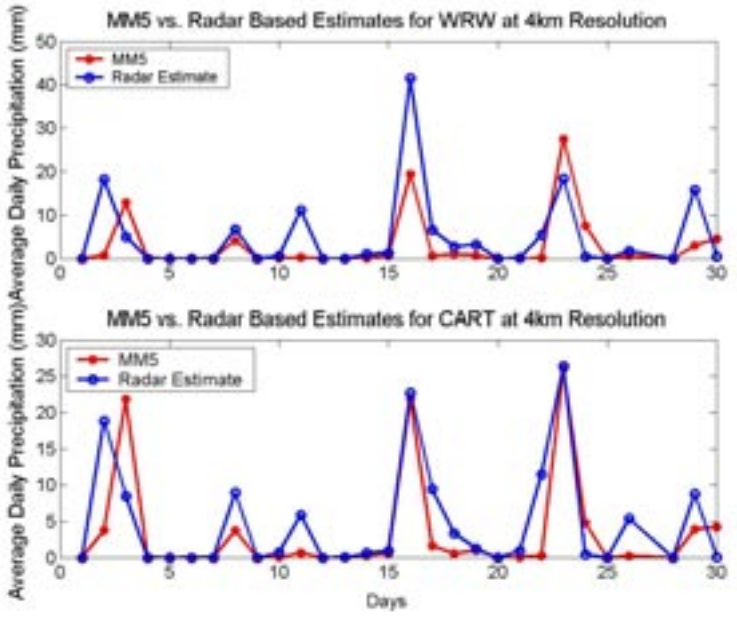

Figure 8. MM5-simulated 4km precipitation and WSR-88D Radar-derived precipitation during March 2000 for A) WRW domain and B) the ARM/CART domain.

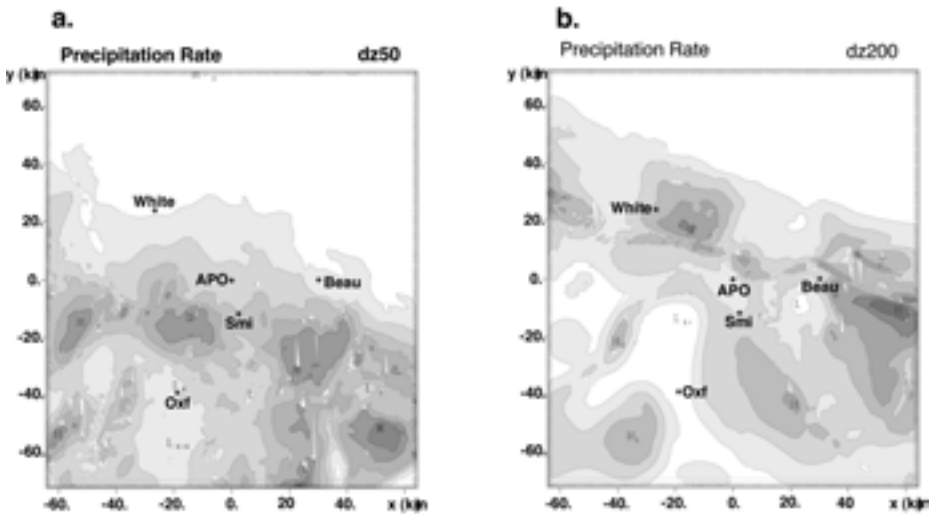

Figure 9. The rainfall rates at 0000 UTC on 3 March 2000, as predicted by the RAMS simulations with 35 vertical levels and 46 vertical levels.

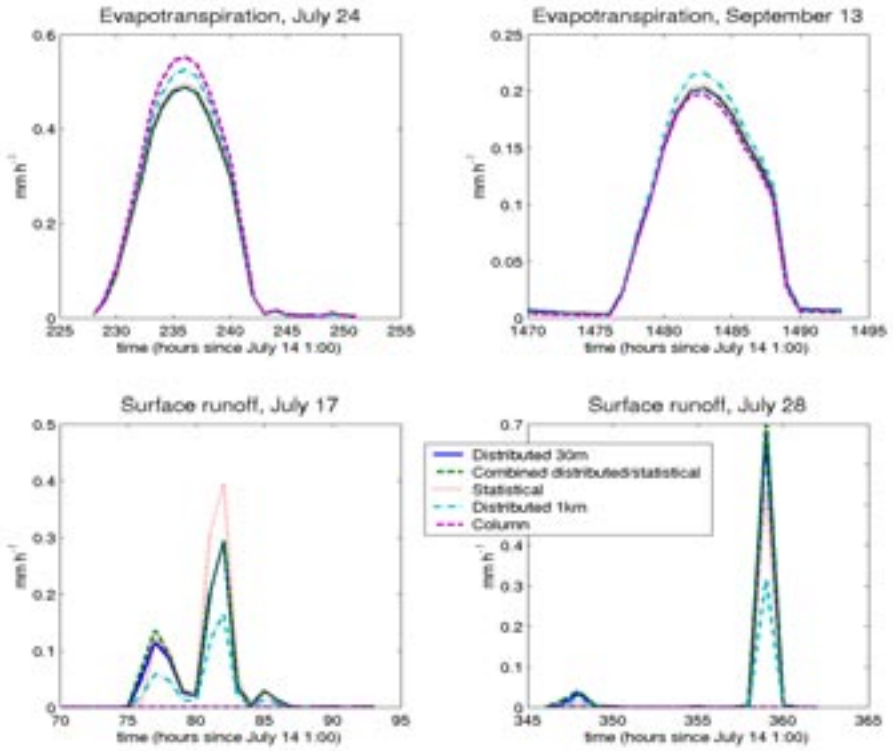

Figure 10. Comparison of the 30m Distributed, Combined Statistical-Distributed, 1km Distributed, and Single Column for A) Evapotranspiration on 24 July, B) Evapotranspiration on 13 September, C) Surface Runoff for 17 July and D) Surface Runoff for 28 July 2000.

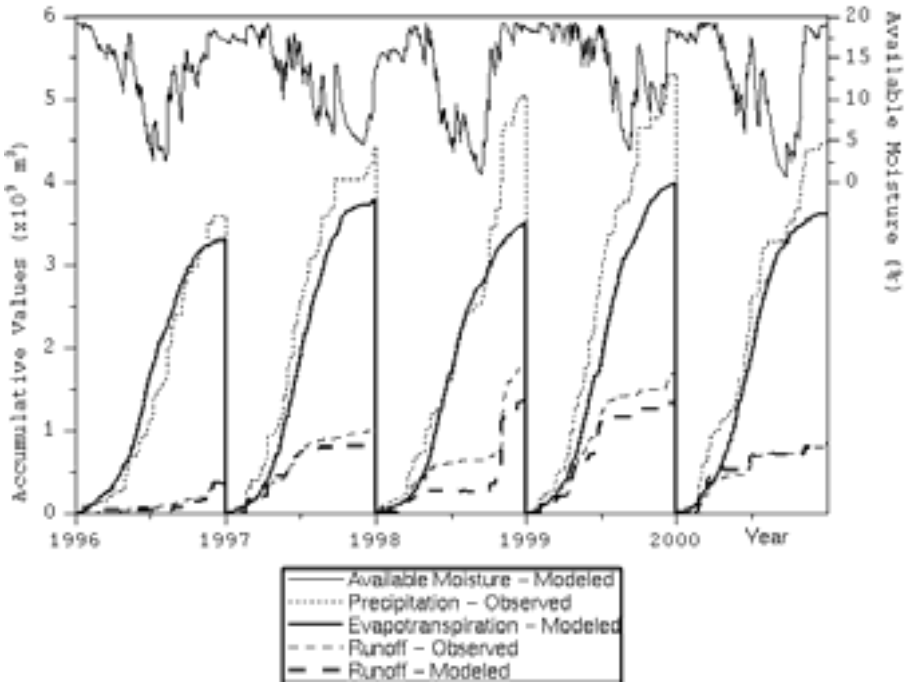

Figure 11. Modeled and observed yearly accumulative values of surface hydrological components at the WRW and modeled root-zone available moisture during 1996-2000.

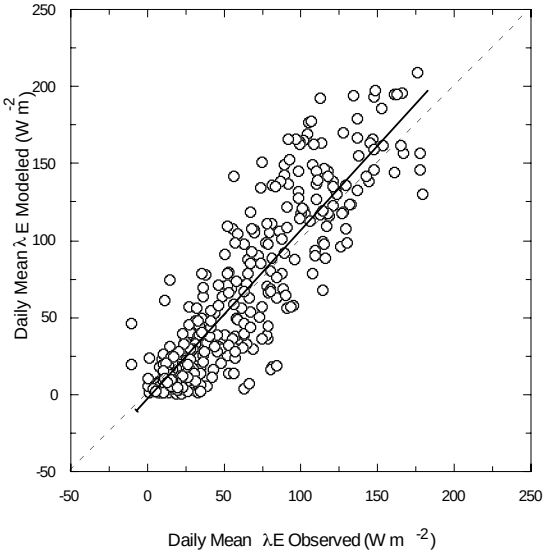

Figure 12. Comparison of modeled versus observed daily mean latent heat fluxes in year 2000 at the Whitewater site. The solid line represents a linear regression fit.

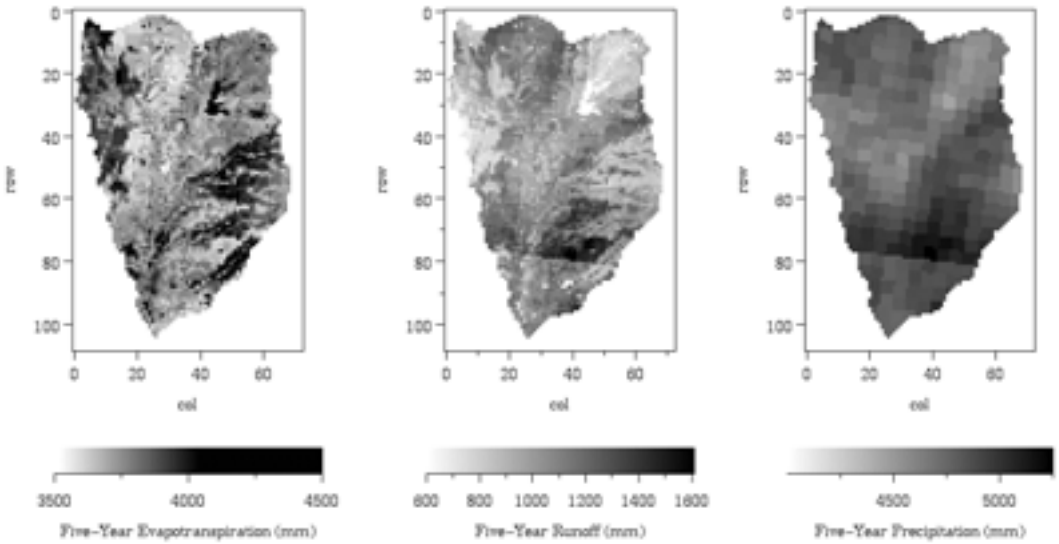

Figure 13. Total modeled evapotranspiration (left), total modeled runoff (center), and observed precipitation (right) for the WRW during 1996-2000.

Vegetation	N	Mean	SE	Minimum	Maximum
Grassland	23	1.77	0.16	0.45	2.95
Pasture	18	1.27	0.33	0.01	5.08
Row Crop	43	2.09	0.13	0.20	3.63
Woodland	25	4.33	0.21	2.17	5.83

Table 1. Licor LAI-2000 leaf area index (LAI) measurements collected in the Whitewater Watershed indicate high variability within each vegetation type.

Vegetation	Mean	Minimum	Maximum
Grassland	2.08	0.43	3.73
Row Crop	2.11	0.46	3.78
Woodland	2.17	0.60	3.77

Table 2. Within-vegetation type spatial variability in predicted LAI for Whitewater Watershed. The minimum is defined by the 10^{th} percentile and the maximum by the 90^{th} percentile of the distribution of LAI values within a vegetation type.

	μ (Radar)/ μ (MM5) [σ(Radar)/ σ(MM5)]		
	4-km	12-km	48-km
WRW	1.68 [1.10]	1.07 [0.68]	1.32 [0.92]
CART	1.41 [1.14]	1.11 [0.84]	1.01 [0.83]

Table 3. Ratios of means and standard deviations between radar-measured and modeled precipitation over the Walnut River Watershed (WRW) and the entire ARM SGP CART site.